



Reusable electrochemical sensor for quinine detection via β -cyclodextrin-based indicator displacement assay

Hanlin Gong, Chenglong Bao, Xuan Luo, Yongsheng Yu, Weiwei Yang*

School of Chemistry and Chemical Engineering, Harbin Institute of Technology, Harbin, Heilongjiang Province 150001, China



ARTICLE INFO

Keywords:

Host-guest interaction
Quinine detection
Electrochemical determination
Electropolymerization
 β -Cyclodextrin
Indicator displacement assay

ABSTRACT

Quinine, a natural alkaloid discovered several centuries ago, has been widely used as an anti-malarial drug and a bitter food additive. However, overconsumption would result in quinine poisoning. Herein, a simple, reusable, and cost-effective electrochemical sensor was presented for quinine detection, utilizing indicator displacement assay (IDA) with β -cyclodextrin/poly(*N*-acetylaniline)/graphene-modified glassy carbon (GC) electrode. Graphene was deposited onto the electrode surface through cyclic voltammetry (CV) electroreduction to enhance the electron transfer properties. The poly(*N*-acetylaniline) film was introduced to inhibit non-special absorption of methylene blue (MB). The β -cyclodextrin (β -CD) molecules were modified on the electrode surface using chronoamperometry to provide a binding site for MB(probe)/quinine(target). Through competitive host-guest interaction, quinine displaced the indicator MB molecule from the β -CD cavity. Differential pulse voltammetry (DPV), cyclic voltammetry (CV), proton nuclear magnetic resonance (^1H NMR), scanning electron microscopy (SEM), electrochemical impedance analysis (EIS), and Fourier transform infrared (FTIR) were employed to verify the successful construction of sensor. The sensor also displayed superior selectivity over the common interfering molecules, satisfactory reusability upon reincubation in MB solution, good reproducibility using the consistent fabrication method, and high stability with an acceptable peak current decrease within 21 days. It is worth pointing out that this is the first time to integrate host-guest recognition with an electrochemical assay for quinine determination. In light of the IDA design strategy, the proposed sensing strategy may inspire innovative engineering methods for molecule detection in the fields of clinical analysis, food safety, and environmental monitoring.

1. Introduction

Quinine, a natural alkaloid extracted from the *cinchona* tree bark, was first isolated by Pelletier and Caventou in 1820 [1]. It is predominantly used as an anti-malaria drug, and occasionally prescribed for lupus, arthritis, and muscle cramps [2]. However, excessive consumption of quinine would induce adverse health effects, such as thrombocytopenia, thrombotic microangiopathy, blindness, and acute kidney injury [3]. The risk of these side effects would be further increased by the use of quinine as a bittering agent in beverages, a practice that necessitates strict regulation [4]. For instance, the United States, Germany, and Greece limit quinine concentrations in drinks to 83 mg/L, 85 mg/L, and 100 mg/L, respectively [5]. Due to its potential toxicity, numerous analytical methods have been developed for the quantitative determination of quinine, including electrochemical techniques [6,7], high-performance liquid chromatography [8,9], colorimetric assay [10],

fluorescence assay [11], and high-resolution mass spectrometry [12]. However, many of these methods suffer from complex functional material preparation, time-consuming operation, extensive consumption of nucleic acid aptamers, or insufficient sensitivity.

In recent years, the quantitative electrochemical methods for quinine analysis have gained increasing attention due to rapid response, operational convenience, affordable instrumentation, and easy miniaturization [2,5,13–15]. For example, Poltorak et al. [13] utilized ion transfer voltammetry (ITV) at the interface between two immiscible electrolyte solutions for quinine detection, proposing a low-cost miniaturization protocol that could be directly translated into a fabricated platform. In another notable study, Du et al. [15] developed a signal-amplifying electrochemiluminescence biosensor, leveraging a nucleic acid signal amplification technique (hybridization chain reaction, HCR) and silver nanoclusters to effectively quantify quinine with a detection limit of 3.7 pM. Despite the accurate determination of quinine achieved by these

* Corresponding author.

E-mail address: yangww@hit.edu.cn (W. Yang).

electrochemical analytical methods, their preparation often necessitates either the specialized device design or the acquisition of costly nucleic acid probes. Therefore, an alternative design method that is simple, reusable, cost-effective, and capable of selective quinine detection is still highly desirable.

The indicator displacement assay (IDA), a significant strategy in supramolecular chemistry for molecular sensing, has been widely utilized for analyte determination by pairing recognition motifs with a signaling unit [16]. The sensing mechanism of IDA is based on the competition between a target analyte and an indicator molecule for the shared binding site on the host. Upon introducing an analyte into a solution containing an “indicator@host” inclusion complex, the analyte takes the place of the indicator from the binding site, resulting in a signal change that facilitates the detection of the analyte [17]. Thus, it is evident that the recognition motifs play an essential role in the sensor fabrication using the IDA design strategy. Indeed, a variety of advanced electrode materials [18–20] and receptor motifs, including cyclodextrin [21,22], cucurbituril [23–25], calixarene [26–28], pillararene [29], and calixpyrrole [30], have been employed in sensor design. As the second-generation macrocyclic molecule, cyclodextrins (CDs) are one of the most commonly utilized recognition motifs due to their commercial availability, relative affordability, and excellent capability. In terms of the number of glucose units, native CDs are classified as α -CD, β -CD, and γ -CD, which can be now obtained via large-scale industrial production [31]. Owing to the feature of hydrophobic inner cavities and hydrophilic exterior cavities [32], CDs can selectively bind special guest molecules by non-covalent interaction, such as Van der Waals forces, hydrogen bonding, and hydrophobic interactions, to form stable host-guest inclusion complexes [33]. Although these unique characteristics position CDs as one of the most promising molecules to fabricate sensors, they typically use fluorescence as a signal output [22,34,35], requiring expensive equipment and limiting practical application.

In this study, a simple, reusable, and cost-effective electrochemical sensor was proposed for quinine detection, based on the IDA design strategy. Methylene blue (MB) and β -cyclodextrin (β -CD) were chosen as the indicator and recognition motif, respectively. Graphene was deposited on the glassy carbon (GC) electrode surface via cyclic voltammetry (CV) electroreduction to enhance the electrode conductivity. The poly(*N*-acetylaniline) film was modified through electro-polymerization to facilitate the immobilization of β -CD and to prevent the non-specific adsorption of MB. Subsequently, the receptor β -CD was installed onto the electrode surface with a facile and controllable electro-oxidation method. Through the host-guest recognition, the MB molecule enters into the hydrophobic inner cavity of β -CD, resulting in the successful construction of a sensor for quinine detection. The physicochemical properties of the β -CD modified GC electrode were examined using electrochemical and surface analytical techniques, confirming the successful preparation of the proposed quinine sensing platform. Various parameters influencing the sensor discrimination of quinine were further investigated to optimize conditions. In the presence of quinine, the decrease in differential pulse voltammetry (DPV) peak current (ΔI) showed a linear relationship with the concentration of quinine. It is worth pointing out that this is the first time to integrate host-guest recognition with an electrochemical assay for quinine determination. The proposed molecular sensing platform offered an alternative, cost-effective method for analyzing small molecules and could potentially be adapted for detecting other molecules by altering the indicator molecules and recognition motifs.

2. Experiment section

2.1. Reagents and chemicals

Graphene oxide (GO) solution (0.5 g/L) was purchased from Shanghai Tanyuanhuigu New Material Technology Company Limited. Quinine, Methylene blue (MB), *N*-acetylaniline, and β -cyclodextrin

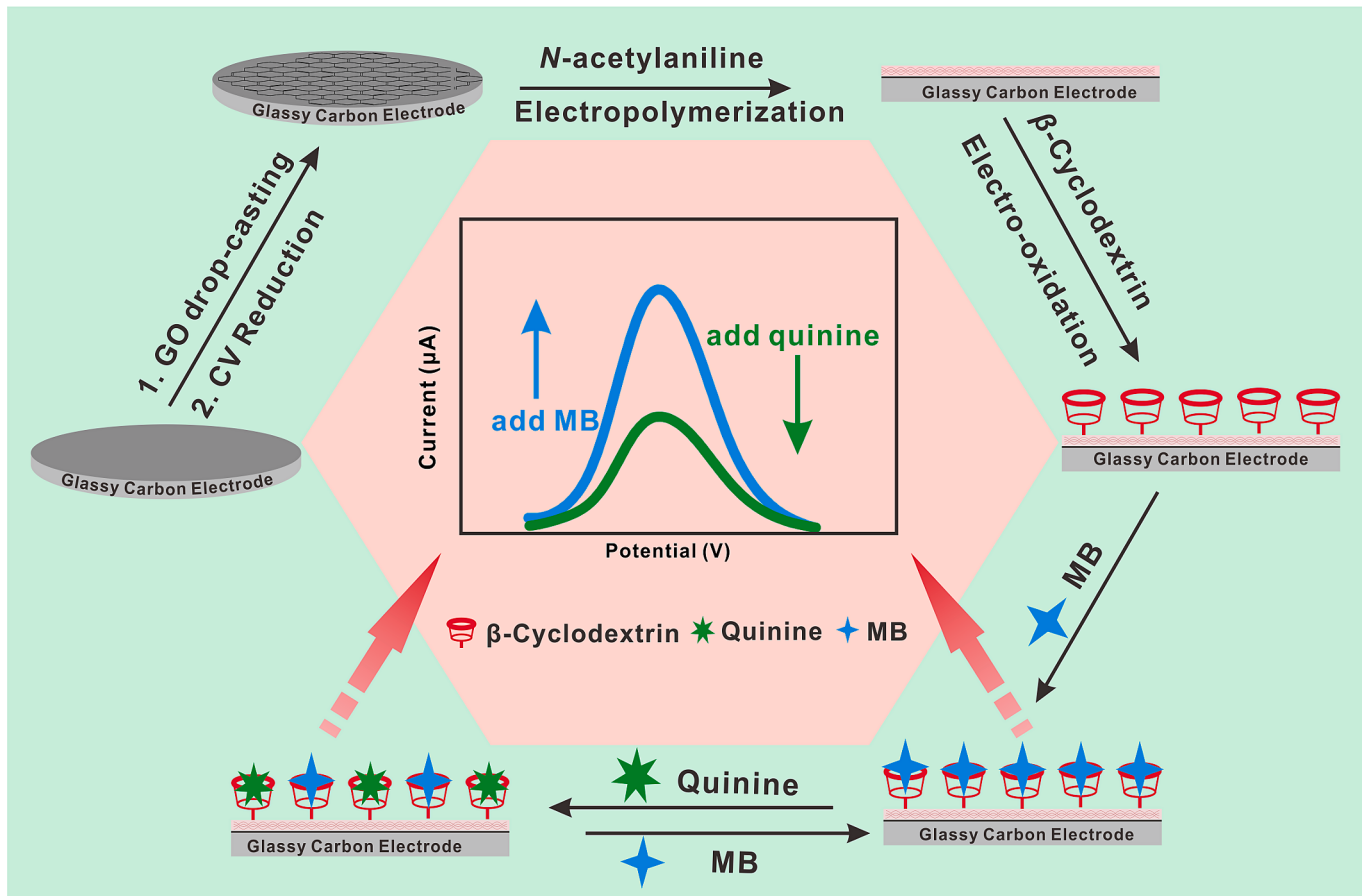
(β -CD) were obtained from Shanghai Aladdin Biochemical Technology Company Limited. Sodium dodecyl sulfate (SDS), ascorbic acid (AA), glycine, bovine serum albumin (BSA), glucose, sucrose, dimethyl formamide (DMF), and tetrabutylammonium perchlorate, were supplied by Beijing InnoChem Science & Technology Company Limited. KCl, MgCl₂, NaClO₄, AgNO₃, HClO₄, Na₂HPO₄·2H₂O, NaH₂PO₄·2H₂O, K₄[Fe(CN)₆]·3H₂O and K₃[Fe(CN)₆] were purchased from Sinopharm Chemical Reagent Company Limited. Phosphate buffer solution (PBS, 0.1 M pH 7.0) was prepared by using Na₂HPO₄·2H₂O and NaH₂PO₄·2H₂O and then was employed as a working solution in electrochemical measurements, if not specifically stated. Since quinine is a hydrophobic molecule with low solubility in water, a 10 mM stock solution of quinine was prepared by dissolving it in ethanol, which was later diluted in 0.1 M PBS for the electrochemical analysis.

2.2. Apparatus

The electrochemical tests (CV, chronoamperometry, and DPV) were carried out using a CHI 1040C Electrochemical Workstation, while electrochemical impedance analysis (EIS) was conducted using the CHI 660E Electrochemical Workstation (Chenhua Instrument Company of Shanghai, China). All electrochemical measurements were performed using a three-electrode system with a platinum wire as the auxiliary electrode, an Ag/AgCl electrode (saturated aqueous KCl solution as the internal reference solution) as the reference electrode, a modified GC electrode with 3 mm diameter as the working electrode. It is important to note that during the electropolymerization of β -CD in DMF solution, the used reference electrode was an Ag⁺/Ag electrode (0.1 M tetrabutylammonium perchlorate and 0.01 M AgNO₃ dissolved in DMF as the internal reference solution). Fourier transform infrared spectroscopy ranging from 400 to 4000 cm⁻¹ was recorded on a PerkinElmer Spectrum 100 FT-IR Spectrometer. ¹H NMR was performed at room temperature on a Bruker ULTRASHIELD 400 operating at 400 MHz. Scanning electron microscopy (SEM) images were obtained using Zeiss Supra55.

2.3. Preparation of the modified electrodes

The fabrication procedure of the quinine sensing platform is depicted in Scheme 1. Before the experiment, the GC electrode was polished carefully using 0.3 μ m Al₂O₃ powder until a mirror-like plane was achieved. It was then rinsed successively with ultrapure water and ethanol for 30 s, followed by sonication. Next, a volume of 5 μ L GO solution (0.1 g/L) was drop-cast onto the GC electrode surface and allowed to dry at ambient temperature. Then, the GO on the electrode surface was reduced by performing CV between -0.3 V and -1.3 V at a scan rate of 0.025 V/s for 10 cycles in a deoxygenated 0.1 M PBS, following a previously reported method [36,37] (named rGO/GC). Subsequently, the rGO/GC electrode was initially subjected to chronoamperometry at a constant voltage of 1.0 V for 90 s and then scanned from -0.2 V to 0.9 V at a scan rate of 0.1 V/s for 30 cycles in a 0.1 M *N*-acetylaniline solution containing 1.0 M HClO₄. The obtained electrode was denoted as pNAANI/rGO/GC and carefully rinsed with ultrapure water. Finally, the β -CD/pNAANI/rGO/GC electrode was prepared by subjecting the pNAANI/rGO/GC electrode to electro-oxidation at a fixed potential of 1.2 V for 900 s in DMF containing 0.1 M β -CD and 0.1 M NaClO₄. The mechanism for β -CD incorporation into the poly(*N*-acetylaniline) film could be attributed to a nucleophilic attack of the highly oxidized conducting poly(*N*-acetylaniline) by the hydroxyl group of β -CD (see Fig. S1 in the Supporting information) [38,39]. It is noted that the β -CD and NaClO₄ DMF solution used in this work was prepared three days in advance. In this work, the other modified electrodes were prepared with a similar procedure for comparison.



Scheme 1. Schematic illustration for the quinine detection based on the host–guest recognition between β -CD and MB (probe)/quinine (target).

2.4. Electrochemical measurements

Before electrochemical detection of quinine, the β -CD/pNAANI/rGO/GC electrode was incubated in a 0.1 M PBS (pH 7.0) containing 10 μ M MB for 35 min to allow MB to enter into the β -CD cavity and then rinsed gently with ultrapure water. This resulting electrode was denoted as MB@ β -CD/pNAANI/rGO/GC. Next, the MB@ β -CD/pNAANI/rGO/GC electrode was immersed in quinine solutions with varying concentrations for 40 min. After incubation in quinine solution, the electrode was taken out of the solution and rinsed with ultrapure water to eliminate any physically adsorbed MB molecules. Finally, DPV was conducted in 0.1 M PBS (pH 7.0), scanning the potential from 0 to -0.5 V with a pulse amplitude of 0.05 V and a pulse width of 0.06 s. EIS and CV were used to characterize the stepwise assembly process on the GC electrode. EIS was carried out in a 5.0 mM $[(Fe(CN)_6)]^{3-/-4-}$ solution containing 0.1 M KCl as the supporting electrolyte, with a frequency from 100 kHz to 0.1 Hz. The interface characterization by CV was conducted in 1 mM $[(Fe(CN)_6)]^{3-/-4-}$ solution containing 0.1 M KCl with scanned range -0.1 V \sim 0.5 V at a scan rate of 0.1 V/s.

The density of the MB enriched on the electrode was confirmed by Formula (1): [40].

$$\Gamma^* = \frac{Q}{nFA} N_A \quad (1)$$

Γ^* is the density of the MB on the electrode surface. Q is the integration of charges under the reduction peaks of CVs with a low scan rate. The constant n is the electron transfer number (the electron transfer number of methylene blue is 2). F represents the Faraday constant. A is the glassy carbon electrode area. N_A represents the Avogadro constant.

The LOD was calculated using the following formula:

$$LOD = 3\sigma/S \quad (2)$$

σ represents the standard deviation of the response signal's noise, and S denotes the slope of the sensor's linear calibration curve.

The t -value was calculated using the following formula:

$$t = \frac{\bar{x} - u_0}{s} \cdot \sqrt{n} \quad (3)$$

\bar{x} is the measured averaged concentration in sample, u_0 is the mean in the null hypothesis, which is the quinine concentration in the soft drink sample, s is the sample standard deviation, n is the sample size, which is 3 in our experiment.

3. Results and discussion

3.1. Feasibility study of the proposed sensor

Scheme 1 presents the design strategy for the proposed electrochemical sensing platform, which is based on the competitive host–guest interaction between β -CD and MB (signal probe)/quinine (target). Because the cavity of β -CD can accommodate MB [41,42], the β -CD-modified electrode exhibits a remarkable DPV peak current after being immersed in MB solution. Additionally, previous studies also indicated that quinine can enter the β -CD cavity to form a stable inclusion complex [43,44]. In the presence of quinine, it would compete with MB for association with the β -CD, thereby displacing MB molecules from the cavities and resulting in a decrease in the DPV peak current. Therefore, by monitoring the changes in DPV signals (ΔI), a quantitative analysis of quinine can be executed.

In order to validate the feasibility of the proposed electrochemical

sensing platform, the DPV response of the modified electrode was first examined in 0.1 M PBS. As shown in Fig. 1, the β -CD/pNAANI/rGO/GC electrode showed no electrochemical signal due to the absence of the indicator molecule MB. However, after incubation with 10 μ M MB solution for 40 min, the MB@ β -CD/pNAANI/rGO/GC electrode displayed a noticeable peak current signal of MB at about -0.24 V. This illustrated that MB molecules entered into the cavities of β -CD. When the MB@ β -CD/pNAANI/rGO/GC electrode was subsequently incubated in a quinine solution for 40 min, a remarkable decrease in peak current was recorded, indicating that MB was replaced by quinine from the β -CD cavity. To further confirm the host-guest interaction between β -CD and MB/quinine, ^1H NMR tests were conducted with a 1:1 M ratio in D_2O . As shown in Fig. S2, after the addition of β -CD, some proton peaks of MB and quinine were both slightly shifted. The shifts of the proton peaks illustrated that MB and quinine can interact with β -CD to form a “guest@host” inclusion complex, which was consistent with previous reports [41,43].

3.2. Characterization of the proposed sensor

The stepwise assembly processes on the GC electrode were characterized using SEM, FTIR spectroscopy, and electrochemical methods. The initial step in preparing the β -CD/pNAANI/rGO/GC electrode involved reducing graphene oxide (GO) through cyclic voltammetry (CV), with the corresponding cyclic voltammograms shown in Fig. S3A. A large reduction peak current was observed in the first cycle, which could be attributed to the reduction of the oxygen groups on GO. As the number of scans increased, the reduction peak current diminished until the scanning curves nearly overlapped, suggesting that the GO was almost fully reduced. The degree of oxygen group removal was further characterized using FTIR spectroscopy. As shown in Fig. S4, several characteristic GO bands were observed, including those at 3371 cm^{-1} , 1729 cm^{-1} , 1622 cm^{-1} , and 1080 cm^{-1} , which represent the stretching vibrations of $-\text{OH}$, $\text{C}=\text{O}$, $\text{C}=\text{C}$, and $\text{C}-\text{O}$ bonds, respectively. After reduction, the band of $\text{C}=\text{O}$ stretch at 1729 cm^{-1} disappeared, and the bands at 1622 cm^{-1} and 1080 cm^{-1} decreased. These results align with previous studies [36], supporting that GO was reduced by CV.

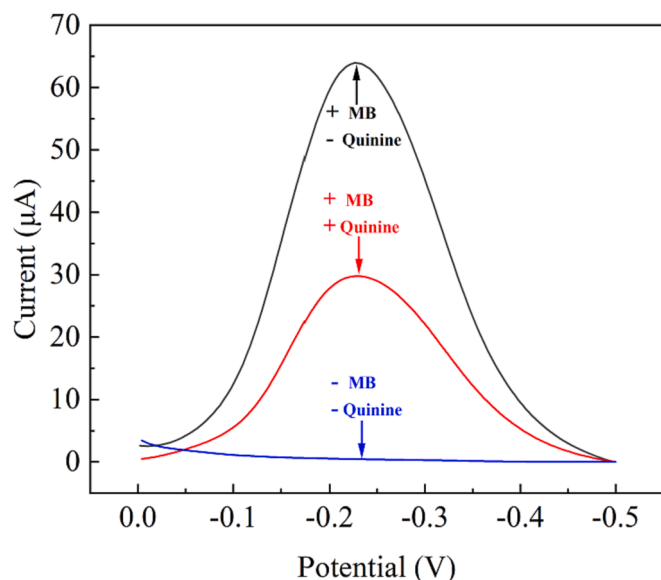


Fig. 1. Feasibility study of the proposed quinine sensing platform. DPV responses of the β -CD/pNAANI/rGO/GC in 0.1 M PBS (blue line), DPV responses after incubation in MB solution for 35 min (black line), and then further incubated in quinine solution for 40 min (red line). (For interpretation of the references to colour in this figure legend, the reader is referred to the web version of this article.)

The morphology characterization of reduced GO was performed using SEM. The resulting image displayed an unevenly corrugated and wrinkled structure (Fig. 2B), a typical morphology of reduced GO and in accordance with reported research [37,45]. In contrast, the surface of the electrode coated with non-reduced GO exhibited a less wrinkled structure because of the hydrophilic nature of GO, which facilitated even distribution (Fig. 2A). Following the preparation of the rGO/GC electrode, the subsequent step was the electropolymerization of *N*-acetylaniline (Fig. S3B and C) and the electro-oxidation of β -CD (Fig. S3D). Because poly(*N*-acetylaniline) film and β -CD were mobilized on the electrode surface, it was difficult to characterize by FTIR spectroscopy. Thus, the pNAANI/rGO/GC and β -CD/pNAANI/rGO/GC electrodes were characterized using SEM. The microstructure image of the poly(*N*-acetylaniline) film showed a significant morphological transformation, with some small dots interspersed on the relatively flat interface (Fig. 2C). Following the electro-oxidation of β -CD onto the pNAANI/rGO/GC electrode, the surface structures of the electrode underwent a marked change. The fabricated sensor interface became densely packed and uniform (Fig. 2D), suggesting the successful assembly of the β -CD/pNAANI/rGO/GC electrode.

The electrochemical characterization of the proposed sensor was also conducted following each preparation step using EIS, CV, and DPV. EIS is a notable and effective technique to characterize the functionalized electrode surface and assess the charge-transfer resistance [46,47]. In the Nyquist plot of EIS, the diameter of the semicircle in the high-frequency regions represents the electron transfer resistance, while the linear region indicates a diffusion-limited process [48]. The results of EIS were shown in Fig. 3A, and the impedance data was fitted based on the Randles equivalent circuit (Inset of Fig. 3A). In this circuit, R_s represents the electrolyte solution resistance, R_{et} represents the surface electron transfer resistance, Z_w represents the Warburg impedance, and C_d represents double layer capacitance. The impedance plot for the bare GC electrode exhibited a small semicircle, with a R_{et} of about $150\ \Omega$, indicating a low electron-transfer resistance. The R_{et} on the rGO/GC electrode decreased remarkably, becoming almost negligible. This could be attributed to the great conductivity of graphene, demonstrating its ability to enhance the electro-transfer capability of the proposed sensing platform. Despite the lack of a noticeable change in the high-frequency region of the Nyquist plot after the modification with the poly(*N*-acetylaniline) film, the corresponding CV result showed a clear increase in peak current (Fig. S5C), indicating the successful construction of the poly(*N*-acetylaniline) film. Owing to the poor conductivity of β -CD molecules, the R_{et} of the β -CD/pNAANI/rGO/GC significantly increased to $1163\ \Omega$. This increase suggested that β -CD molecules were immobilized on the electrode. CV was further employed to substantiate the results obtained from EIS (Fig. S5). Fig. S5A showed a well-defined reversible redox pair of $[\text{Fe}(\text{CN})_6]^{3-/4-}$ at the bare GC electrode. A notable increase in peak current was observed, attributed to the superior electrical conductivity of graphene, as shown in Fig. S5B. Following the electropolymerization of the poly(*N*-acetylaniline) film on the electrode surface, the CV curve underwent a significant transformation and the redox peak of $[\text{Fe}(\text{CN})_6]^{3-/4-}$ became less distinct (Fig. S5C). However, the CV peak current showed a decrease after the installation of poorly conductive β -CD molecules (Fig. S5D), supporting the β -CD modification on the pNAANI/rGO/GC electrode. The CV results were in agreement with those obtained from EIS analysis and these two analytical techniques both confirmed the successful preparation of the CD/pNAANI/rGO/GC electrode.

Fig. 3B showed the DPV responses of various electrodes after incubation in a 10 μ M MB solution. A modest and smooth peak current was observed on the bare GC electrode, attributable to the physical adsorption of MB on the electrode surface. After the deposition of reduced GO onto the GC electrode, a larger peak current was noted, due to the larger surface area provided by the wrinkled graphene and the π - π stacking interaction between MB and graphene. However, virtually no peak current was visible on the pNAANI/rGO/GC electrode surface,

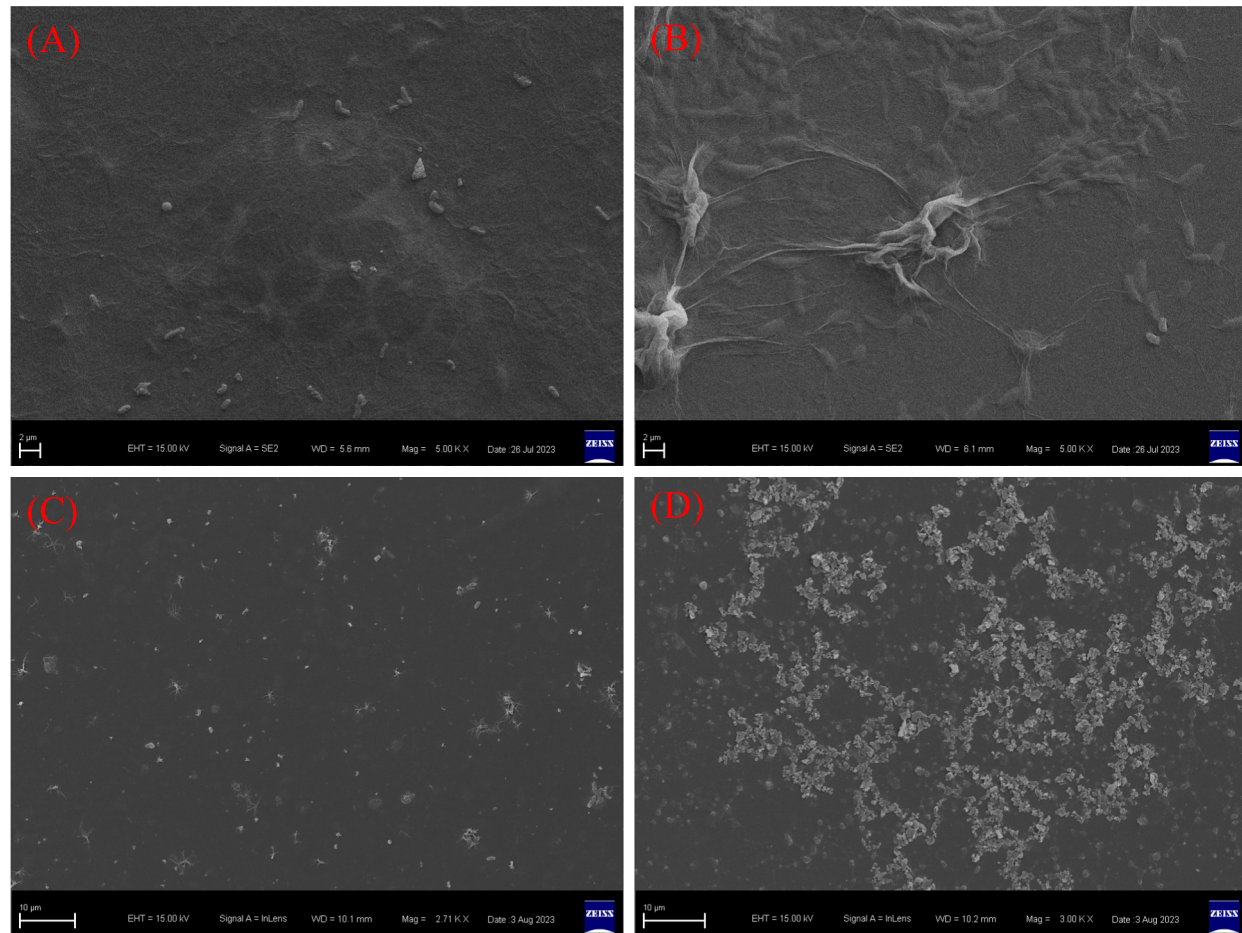


Fig. 2. The morphology characterization of the stepwise assembly processes on the GC electrode. (A) The SEM images of GO/GC, (B) rGO/GC, (C) pNAANI/rGO/GC, and (D) β -CD/pNAANI/rGO/GC.

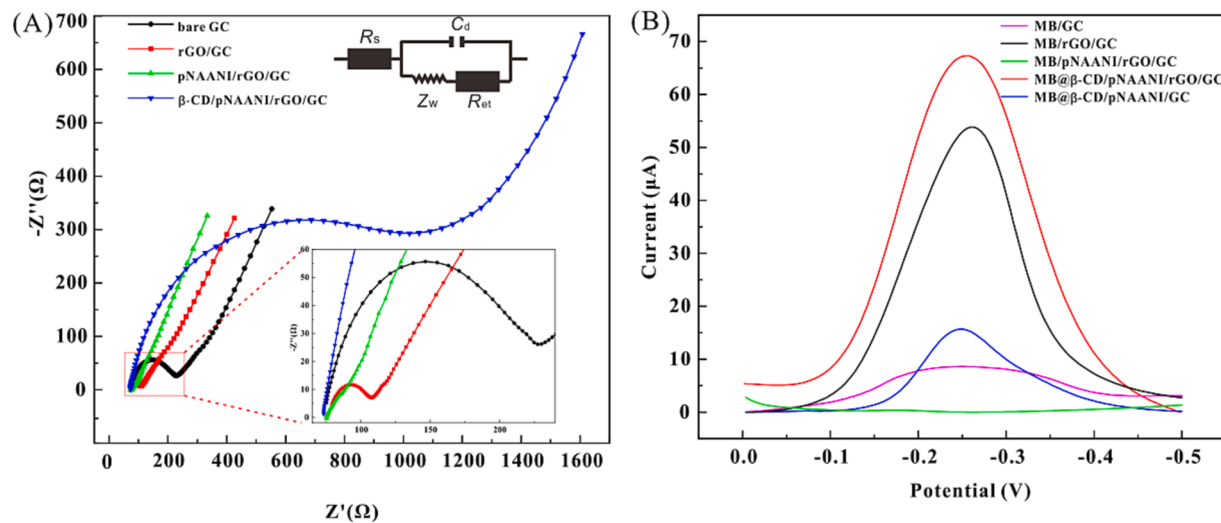


Fig. 3. The electrochemical characterization of the stepwise assembly processes on the GC electrode. (A) The EIS characterization carried out in 5.0 mM $[(\text{Fe}(\text{CN})_6)]^{3-/4-}$ solution containing 0.1 M KCl supporting electrolyte with the frequency from 100 kHz to 0.1 Hz, and (B) the DPV characterization carried out in 0.1 M PBS (pH 7.0).

suggesting that the non-specific adsorption of MB was restrained by the poly(*N*-acetylaniline) film. Furthermore, the peak current on the β -CD/pNAANI/rGO/GC showed a significant increase, due to the good host-guest recognition property and high enrichment capability of β -CD.

To ascertain the effect of graphene on sensor performance, a control experiment was performed on β -CD/pNAANI/GC. As expected, a lower DPV signal than that of β -CD/pNAANI/rGO/GC was observed, implying that the large specific surface area and superior electron transfer

property of graphene could enhance the electrochemical performance of the proposed sensor. In summary, graphene improved the electron transfer of the developed sensing platform, and the poly(*N*-acetylani-line) film successfully minimized the non-specifical adsorption of MB on the electrode surface.

3.3. Optimization of experimental conditions

After demonstrating the feasibility of the sensing strategy and characterizing the sensor, several control experiments including the cycle number of the *N*-acetylaniline electropolymerization, the electro-oxidation time of β -CD, and the incubation time of β -CD/pNAANI/rGO/GC in MB/quinine solution was conducted, to enable high-performance detection of quinine with the established sensing platform. Fig. 4A showed the impact of the cycle number of the *N*-acetylaniline electropolymerization on the DPV peak current of the pNAANI/rGO/GC in 0.1 M PBS after incubation in a 10 μ M MB solution. As the number of cycles increased, the reduction peak current of MB gradually decreased and reached an approximate value of 0 at 30 cycles. This observation indicated that the rGO/GC electrode surface was fully covered by the poly(*N*-acetylaniline) film and that the pNAANI/rGO/GC electrode effectively can avoid the non-specific adsorption of MB. Therefore, 30 cycles were chosen for the subsequent experiment. According to the electro-oxidation mechanism of β -CD on the electrode

surface (Fig. S1), the electro-oxidation time of β -CD is crucial to enhance the sensitivity and recognition capability of the sensor because the deposition time directly influences the quantity of β -CD molecules on the electrode surface. Therefore, the electro-oxidation time of β -CD was also optimized. Fig. 4B showed that the current response increased with the deposition time, reaching an optimal value at 15 min. This suggested that the maximum amount of β -CD was installed on the electrode at this point. Consequently, 15 min was chosen as the optimal deposition time for further experiments. In addition, the incubation time of the β -CD/pNAANI/rGO/GC electrode in MB solution is also an important parameter. Due to the host-guest recognition between the MB and β -CD molecule, the DPV peak current increased with the incubation time in the MB solution, reaching a stable value at 35 min (Fig. 4C). This indicated that the enrichment of MB on β -CD/pNAANI/rGO/GC electrode surface reached saturation. The number of probe MB on the saturated sensor surface was calculated with Formula (1) and the result of 1.18×10^{15} molecules/cm² was obtained (the corresponding CV tests in Fig. S6). Because the process of replacing MB from the cavity of β -CD is time-dependent, necessitating the optimization of incubation time in quinine solution to achieve accurate sensor responses. Thus, the incubation time of the MB@ β -CD/pNAANI/rGO/GC electrode in a 50 μ M quinine solution was also examined (Fig. 4D). It was observed that the DPV signal stabilized after an incubation period of 40 min. Therefore, 40 min was selected as the optimal incubation time for the prepared

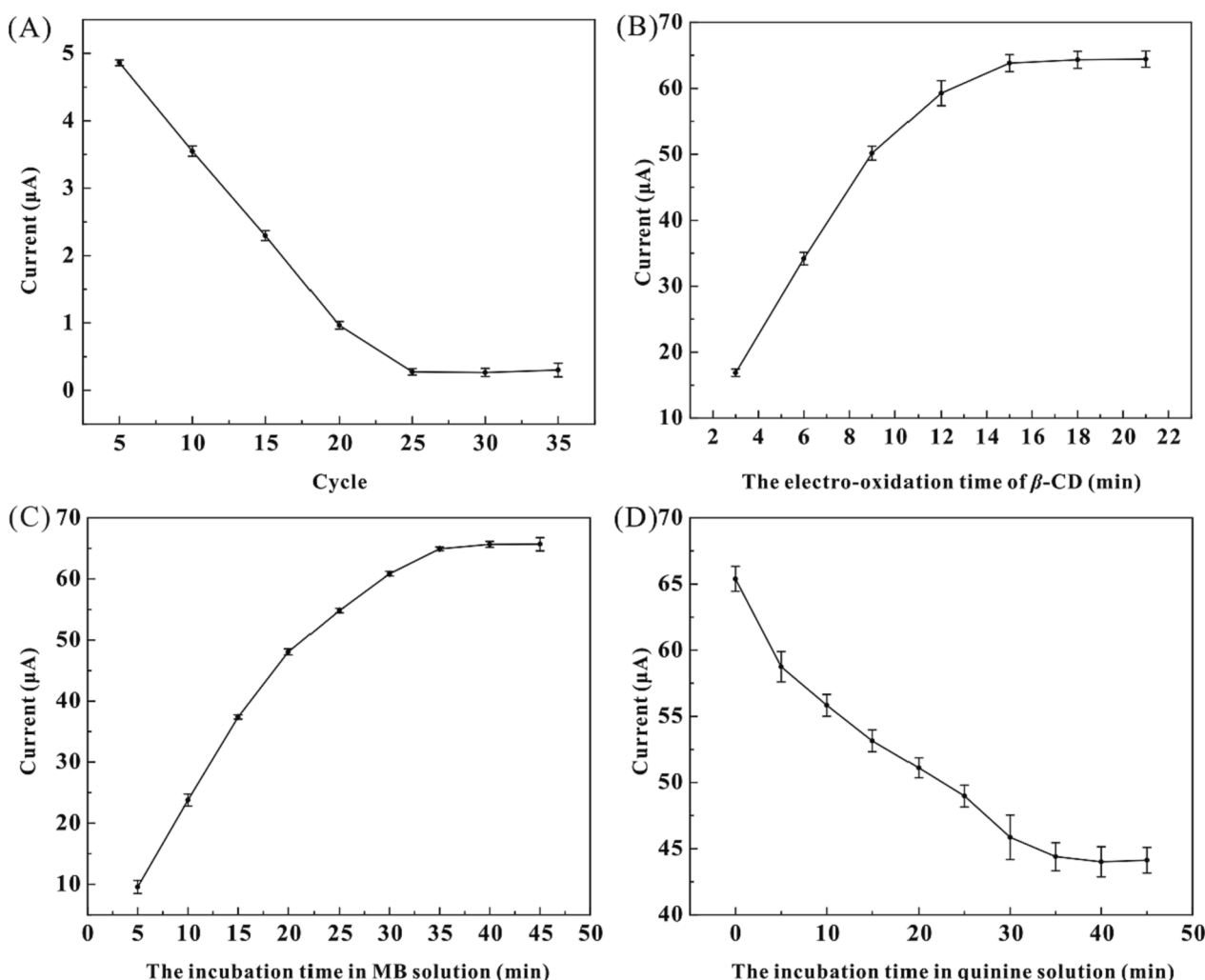


Fig. 4. Optimization of experimental conditions. (A) Effect of the cycle number of the CV for 0.1 M *N*-acetylaniline deposition, (B) effect of the electro-oxidation time of β -CD by chronoamperometry in DMF containing 0.1 M β -CD and 0.1 M NaClO_4 , (C) effect of incubation time in 10 μ M MB solution, (D) effect of incubation time in 50 μ M quinine solution after incubation in MB solution.

electrode in the quinine solution. In addition, graphs corresponding to all optimization experiments were also shown in Fig. S7. After optimizing the experimental parameters, the ideal sensing conditions were determined as follows: the cycle number for *N*-acetylaniline electro-polymerization was set as 30 cycles, the β -CD immobilization time was set as 15 min, the incubation time in the MB solution was 35 min, and the incubation time in the quinine solution was 40 min.

3.4. Quantitative analysis of the sensor toward quinine

Under the optimized conditions, the quantitative determination of quinine was carried out using DPV, and the corresponding results were shown in Fig. 5. It is seen that the MB probe in β -CD cavities was replaced gradually with the increase of quinine, causing a gradual decrease in the reduction peak current of MB (Fig. 5A). This was observed across a range of quinine concentrations from 0 nM to 125 μ M. As shown in Fig. 5B, There was a linear increase in ΔI_{MB} with the rise in quinine concentration. The corresponding linear function was ΔI_{MB} (μ A) = $1.585 + 0.382C$ (μ M) ($R^2 = 0.998$) and the limit of detection (LOD) was 1.32 μ M, according to the calculation of Formula (2). Table S1 compares the analytical performances of some electrochemical methods reported for quinine detection. In general, the detection limit and sensitivity of the proposed sensing strategy are satisfactory and the proposed sensor holds promising potential for the electrochemical determination of quinine in tonic water or contaminated organic wastewater.

3.5. Selectivity, reusability, reproducibility stability and repeatability

As is widely acknowledged, real samples contain a variety of molecules that may interfere with quinine detection, potentially compromising the selectivity of the electrochemical sensor. Consequently, the selectivity of the proposed sensing platform was investigated, using over ten-fold the concentration of other common molecules. Fig. 6A revealed that KCl (1.0 mM), MgCl₂ (1.0 mM), sodium dodecyl sulphate (SDS, 1.0 mM), ascorbic acid (AA, 1.0 mM), glucose (1.0 mM), sucrose (1.0 mM), glycine (1.0 mM), and bovine serum albumin (BSA, 1.0 mg/mL) had negligible interference when compared to the detection of quinine at a mere 75 μ M concentration. Due to the reversibility of competitive host-guest interaction, the reusability of the proposed sensing platform was studied by reincubation in the MB solution. The prepared sensor was initially immersed in 30 μ M quinine solution for 45 min and then reincubated in 10 μ M MB solution for 35 min. As shown in Fig. 6B, the developed sensing platform displayed good regeneration capabilities and the sensor could be reused several times. Additionally, the stability

of the proposed sensor was scrutinized through storage at 4 °C, with the results illustrated in Fig. 6C. A negligible change in the DPV signal was observed during the initial seven days. Despite a decrease in the signal commencing on the eighth day, it retained 86.47 % of its original value up until the 21st day. In addition, the reproducibility of the proposed sensor was assessed by measuring the DPV peak current following incubation in a 10 μ M MB solution. Seven identical MB@ β -CD/pNAANI/rGO/GC electrodes displayed similar signals with a relative standard deviation of 2.06 %, indicating good reproducibility of the developed sensor (Fig. 6D). Lastly, the repeatability of the sensor also performed to ascertain the inter-electrode consistency. Five independent fabrication MB@ β -CD/pNAANI/rGO/GC electrodes were used to detect 30 μ M quinine solution. As shown in Fig. S8, five electrodes displayed similar signals with a relative standard deviation of 0.5 %, indicating good repeatability of the developed sensor. Overall, these findings demonstrated the proposed sensor's satisfactory selectivity, reusability, stability, reproducibility and repeatability.

3.6. Analytical application in soft drinks

To evaluate the potential real-world application of the proposed sensor, MB@ β -CD/pNAANI/rGO/GC electrode was employed to detect quinine in an actual beverage sample using the standard addition method. The soft drinks were purchased from a local supermarket without any further treatment, to which specific quantities of quinine were added. As shown in Table 1, the recoveries of quinine were from 98.3 % to 109.3 %, with relative errors (RSD) varying between 0.83 % and 1.95 %. Relative errors were defined as δ/M , where δ represents the standard deviation of the measured quinine concentration and M denotes the corresponding mean value. The t-values were calculated according to the Formula (3). Looking up the Critical Values of the t Distribution ($t_{0.01/2} = 9.925$, two-tails), the outcome of this statistical comparison substantiated that there are no significant discrepancies, thereby demonstrating the potential of the proposed sensing platform for widespread and practical applications in real-world samples.

4. Conclusions

In summary, a novel, reusable, and cost-effective electrochemical sensing platform was successfully engineered for quinine detection based on IDA strategy using a β -CD functionalized GC electrode. In this work, graphene initially was electrochemically reduced and deposited onto the electrode surface to enhance its electron transfer properties. Subsequently, the poly(*N*-acetylaniline) film was modified on the electrode surface through electropolymerization to prevent the non-

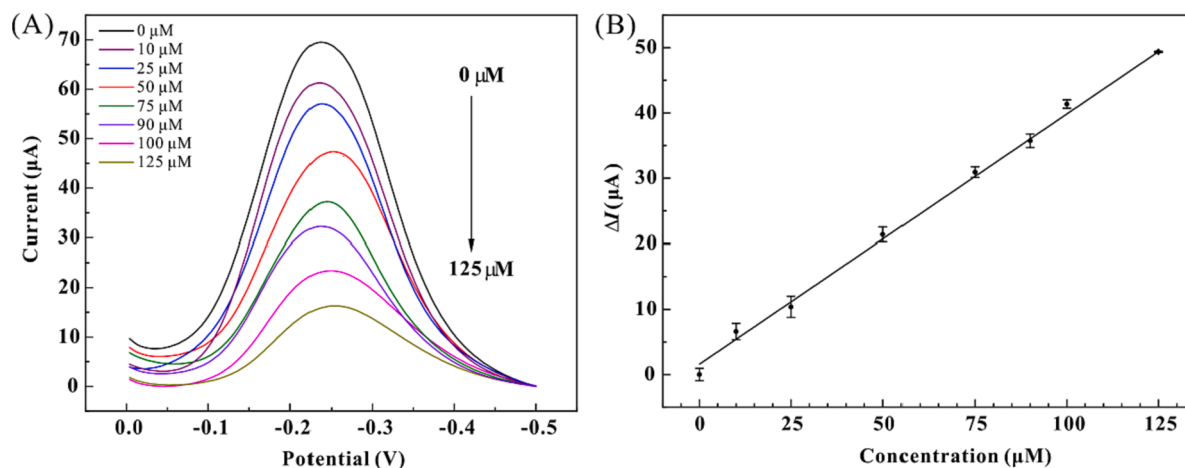


Fig. 5. Quantitative analysis of the sensor toward quinine. (A) DPV responses recorded at MB@ β -CD/pNAANI/rGO/GC in 0.1 M PBS upon adding of quinine (from 0 μ M to 125 μ M), (B) the calibration plots of the peak current response versus concentrations of quinine.

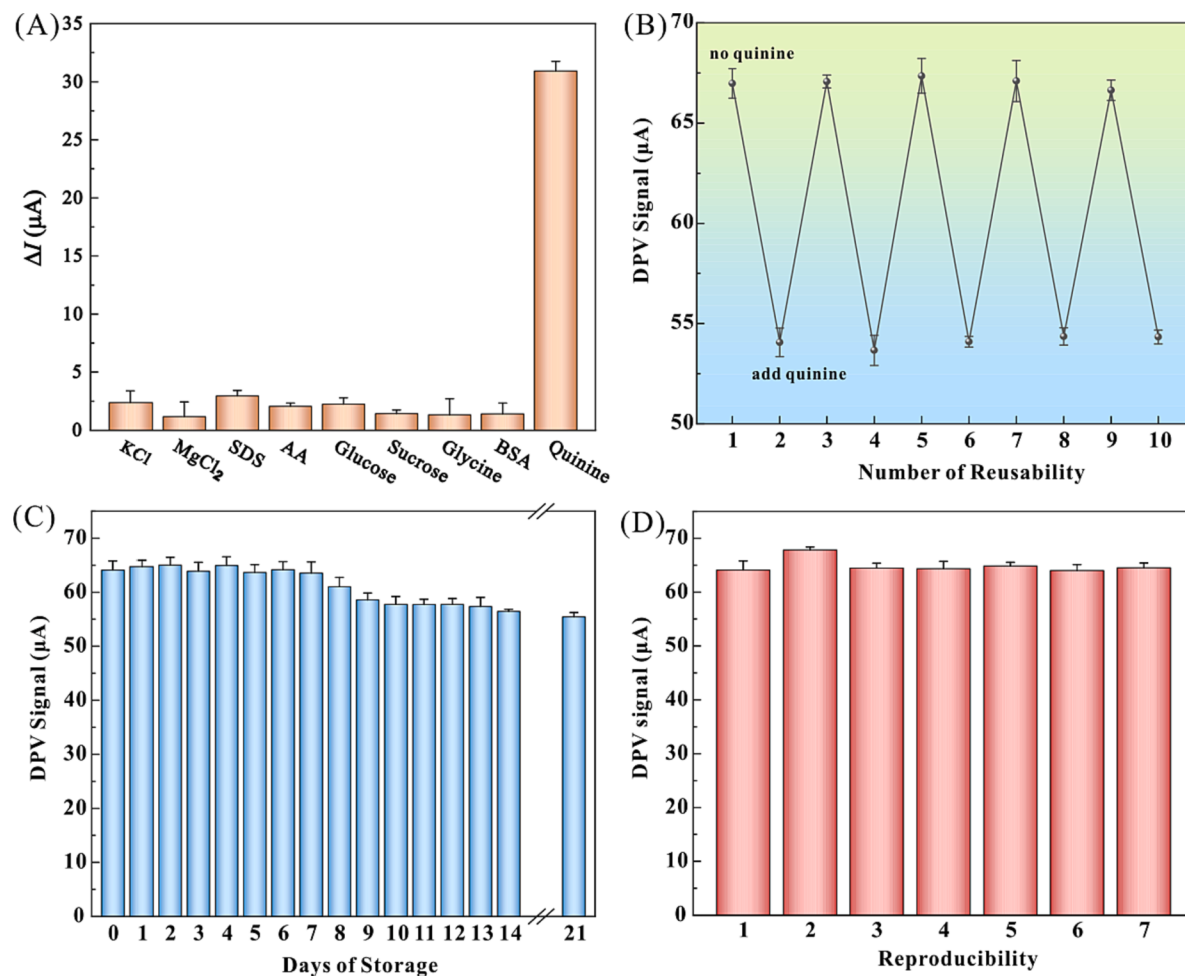


Fig. 6. (A) The selectivity studies of the developed sensor using different species and 75 μM vs 1 mM other substances; (B) Typical interrogation-regeneration plots of the proposed quinine sensor with the stepwise challenge with 30 μM quinine then incubated with the MB; (C) The stability studies of the developed sensor storing the sensor at 4 °C; (D) The reproducibility studies of the developed sensor.

Table 1
Measurement results of quinine in soft drinks.

Sample	Added/ μM	Founded/ μM	Number of determinations (n)	RSD/%	Recovery/%	t-value
1	30	32.80 ± 0.64	3	1.95	109.3	7.5
2	50	48.72 ± 1.27	3	2.62	97.4	1.74
3	100	98.26 ± 0.81	3	0.83	98.3	3.72
blank	0	0.27 ± 1.47	3	/	/	0.32

absorption of MB. The β -CD, successfully modified on the sensor interface, displayed excellent host-guest recognition capabilities. Under optimum conditions, the developed sensor exhibited a satisfactory analytical performance for the electrochemical detection of quinine. The linear response range of the proposed sensor was 10–125 μM with a low detection limit of 1.32 μM . Additionally, the developed sensing platform displayed superior selectivity over the common interfering molecules, satisfactory reusability upon reincubation in MB solution, good reproducibility using the consistent fabrication method, and high stability with a negligible peak current decrease within seven days. The impressive analytical performance of the proposed sensor in real sample testing demonstrated its potential applications. Overall, the integration of host-guest recognition and electrochemical assay provides a promising approach for quinine detection and may inspire innovative engineering methods for molecule detection in the fields of food safety, clinical analysis, and environmental monitoring.

CRediT authorship contribution statement

Hanlin Gong: Investigation, Conceptualization, Methodology, Formal analysis, Data curation, Resources, Writing – original draft, Writing – review and editing, Supervision, Project administration. **Chenglong Bao:** Formal analysis. **Xuan Luo:** Formal analysis. **Yongsheng Yu:** Funding acquisition. **Weiwei Yang:** Resources, Writing – original draft, Writing – review and editing, Visualization, Investigation, Validation, Supervision, Project administration, Funding acquisition.

Declaration of competing interest

The authors declare that they have no known competing financial interests or personal relationships that could have appeared to influence the work reported in this paper.

Data availability

Data will be made available on request.

Acknowledgments

This work was supported by the National Natural Science Foundation of China under Grant (No. 21305025), the Fundamental Research Funds for the Central Universities (HIT.OCEF.2021025), State Key Laboratory of Urban Water Resource and Environment (Harbin Institute of Technology, No. ES202211) and Heilongjiang Science Foundation (No. LH2020B006).

Appendix A. Supplementary data

Supplementary data to this article can be found online at <https://doi.org/10.1016/j.microc.2024.110109>.

References

- [1] R.F. Dawson, Quinine and quinidine production in the Americas: a brief history, *HortTechnology* 1 (1991) 17–20, <https://doi.org/10.21273/HORTTECH.1.1.17>.
- [2] O. Dushna, L. Dubenska, M. Marton, M. Hatala, M. Vojs, Sensitive and selective voltammetric method for determination of quinoline alkaloid, quinine in soft drinks and urine by applying a boron-doped diamond electrode, *Microchem. J.* 191 (2023) 108839–108849, <https://doi.org/10.1016/j.microc.2023.108839>.
- [3] N.W. Liles, E.E. Page, A.L. Liles, S.K. Vesely, G.E. Raskob, J.N. George, Diversity and severity of adverse reactions to quinine: a systematic review, *Am. J. Hematol.* 91 (2016) 461–466, <https://doi.org/10.1002/ajh.24314>.
- [4] V.C. Tsafafari, M. Tarara, P.D. Tzanavaras, G.Z. Tsogas, A novel equipment-free paper-based fluorometric method for the analytical determination of quinine in soft drink samples, *Sensors* 23 (2023) 5153–5163, <https://doi.org/10.3390/s23115153>.
- [5] Y. Qiu, C. Gu, B. Li, H. Shi, Aptamer detection of quinine in reclaimed wastewater using a personal glucose meter, *Anal. Methods* 10 (2018) 2931–2938, <https://doi.org/10.1039/c8ay00585k>.
- [6] L. Li, F. Tian, L. Qiu, F. Wu, W. Yang, Y. Yu, Recent Progress on Ruthenium-Based Electrocatalysts towards the Hydrogen Evolution Reaction, *Catalysts* 13 (2023) 1497, <https://doi.org/10.3390/catal13121497>.
- [7] X. Guo, L. Qiu, M. Li, F. Tian, X. Ren, S. Jie, S. Geng, G. Han, Y. Huang, Y. Song, W. Yang, Y. Yu, Accelerating the generation of NiOOH by in-situ surface phosphating nickel sulfide for promoting the proton-coupled electron transfer kinetics of urea electrolysis, *Chem. Eng. J.* 483 (2024) 149264, <https://doi.org/10.1016/j.cej.2024.149264>.
- [8] L. Chmurzynski, High-performance liquid chromatographic determination of quinine in rat biological fluids, *J. Chromatogr. B* 693 (1997) 423–429, [https://doi.org/10.1016/S0378-4347\(97\)00074-1](https://doi.org/10.1016/S0378-4347(97)00074-1).
- [9] V.F. Samanidou, E.N. Evangelopoulou, I.N. Papadoyannis, Simultaneous determination of quinine and chloroquine anti-malarial agents in pharmaceuticals and biological fluids by HPLC and fluorescence detection, *J. Pharm. Biomed. Anal.* 38 (2005) 21–28, <https://doi.org/10.1016/j.jpba.2004.12.005>.
- [10] Y. Ahmadi, R. Soldo, K. Rathammer, L. Ebler, I. Barisic, Analyzing criteria affecting the functionality of g-quadruplex-based DNA aptazymes as colorimetric biosensors and development of quinine-binding aptazymes, *Anal. Chem.* 93 (2021) 5161–5169, <https://doi.org/10.1021/acs.analchem.0c05052>.
- [11] T.-Y. Liu, X.-L. Qu, B. Yan, A sensitive metal-organic framework nanosensor with cation-introduced chirality for enantioselective recognition and determination of quinine and quinidine in human urine, *J. Mater. Chem. C* 8 (2020) 14579–14586, <https://doi.org/10.1039/d0tc03952g>.
- [12] S. Martinez-Jarquin, A. Begley, Y.H. Lai, G.L. Bartolomeo, A. Pruska, C. Rotach, R. Zenobi, Aptapaper—an aptamer-functionalized glass fiber paper platform for rapid upconcentration and detection of small molecules, *Anal. Chem.* 94 (2022) 5651–5657, <https://doi.org/10.1021/acs.analchem.2c00035>.
- [13] K. Rudnicki, K. Sobczak, P. Borgul, S. Skrzypek, L. Poltorak, Determination of quinine in tonic water at the miniaturized and polarized liquid-liquid interface, *Food Chem.* 364 (2021) 130417–130424, <https://doi.org/10.1016/j.foodchem.2021.130417>.
- [14] M. Buleandra, A.A. Rabinca, M.C. Cheregi, A.A. Ciucu, Rapid voltammetric method for quinine determination in soft drinks, *Food Chem.* 253 (2018) 1–4, <https://doi.org/10.1016/j.foodchem.2018.01.130>.
- [15] Y. Liu, H. Bian, Y. Wu, Y. Yin, J. Wu, Z. Peng, J. Du, Ultrasensitive electrochemiluminescence biosensors based on programmable aptazyme-induced hybridization chain reaction for detecting adenosine triphosphate and quinine, *Sens. Actuators B Chem.* 369 (2022) 132266–132275, <https://doi.org/10.1016/j.snb.2022.132266>.
- [16] A.C. Sedgwick, J.T. Brewster, T. Wu, X. Feng, S.D. Bull, X. Qian, J.L. Sessler, T. D. James, E.V. Anslyn, X. Sun, Indicator displacement assays (IDAs): the past, present and future, *Chem. Soc. Rev.* 50 (2021) 9–38, <https://doi.org/10.1039/c9cs00538b>.
- [17] L. Yang, X. Ran, L. Cai, Y. Li, H. Zhao, C.P. Li, Calix[8]arene functionalized single-walled carbon nanohorns for dual-signalling electrochemical sensing of aconitine based on competitive host-guest recognition, *Biosens. Bioelectron.* 83 (2016) 347–352, <https://doi.org/10.1016/j.bios.2016.04.079>.
- [18] Z. Mirzaei Karazan, M. Roushani, Electrochemical determination of mercury ions in different food samples using glassy carbon electrode modified with poly (crocin), *Microchem. J.* 195 (2023) 109402–109409, <https://doi.org/10.1016/j.microc.2023.109402>.
- [19] M. Roushani, E. Karami, A. Salimi, R. Sahraei, Amperometric detection of hydrogen peroxide at nano-ruthenium oxide/riboflavin nanocomposite-modified glassy carbon electrodes, *Electrochim. Acta* 113 (2013) 134–140, <https://doi.org/10.1016/j.electacta.2013.09.069>.
- [20] N.H. Sibit, M. Roushani, Z.M. Karazan, Electrochemical determination of mercury ions in various environmental samples using glassy carbon electrode modified with poly (L-tyrosinamide), *Ionics* (2023), <https://doi.org/10.1007/s11581-023-05334-y>.
- [21] D. Wu, L. Tan, C. Ma, F. Pan, W. Cai, J. Li, Y. Kong, Competitive self-assembly interaction between ferrocenyl units and amino acids for entry into the cavity of β-cyclodextrin for chiral electroanalysis, *Anal. Chem.* 94 (2022) 6050–6056, <https://doi.org/10.1021/acs.analchem.2c00777>.
- [22] Y. Suzuki, Y. Mizuta, A. Mikagi, T. Misawa-Suzuki, Y. Tsuchido, T. Sugaya, T. Hashimoto, K. Ema, T. Hayashita, Recognition of d-glucose in water with excellent sensitivity, selectivity, and chiral selectivity using gamma-cyclodextrin and fluorescent boronic acid inclusion complexes having a pseudo-diboronic acid moiety, *ACS Sens.* 8 (2023) 218–227, <https://doi.org/10.1021/acssensors.2c02087>.
- [23] J. Kramer, L.M. Grimm, C. Zhong, M. Hirtz, F. Biedermann, A supramolecular cucurbit[8]uril-based rotaxane chemosensor for the optical tryptophan detection in human serum and urine, *Nat. Commun.* 14 (2023) 518–532, <https://doi.org/10.1038/s41467-023-36057-3>.
- [24] C. Hu, T. Jochmann, P. Chakraborty, M. Neumaier, P.A. Levkin, M.M. Kappes, F. Biedermann, Further dimensions for sensing in biofluids: distinguishing bioorganic analytes by the salt-induced adaptation of a cucurbit[7]uril-based chemosensor, *J. Am. Chem. Soc.* 144 (2022) 13084–13095, <https://doi.org/10.1021/jacs.2c01520>.
- [25] N.M. Kumar, P. Picchetti, C. Hu, L.M. Grimm, F. Biedermann, Chemiluminescent cucurbit[n]uril-based chemosensor for the detection of drugs in biofluids, *ACS Sens.* 7 (2022) 2312–2319, <https://doi.org/10.1021/acssensors.2c00934>.
- [26] Z. Zheng, H. Yu, W.C. Geng, X.Y. Hu, Y.Y. Wang, Z. Li, Y. Wang, D.S. Guo, Guanidinocalix[5]arene for sensitive fluorescence detection and magnetic removal of perfluorinated pollutants, *Nat. Commun.* 10 (2019) 5762–5770, <https://doi.org/10.1038/s41467-019-13775-1>.
- [27] Y. Zhang, H. Yu, S. Chai, X. Chai, L. Wang, W.C. Geng, J.J. Li, Y.X. Yue, D.S. Guo, Y. Wang, Noninvasive and individual-centered monitoring of uric acid for precaution of hyperuricemia via optical supramolecular sensing, *Adv. Sci. N. S.* 9 (2022) 2104463–2104472, <https://doi.org/10.1002/advs.202104463>.
- [28] H. Yu, X. Chai, W.C. Geng, L. Zhang, F. Ding, D.S. Guo, Y. Wang, Facile and label-free fluorescence strategy for evaluating the influence of bioactive ingredients on fmo3 activity via supramolecular host-guest reporter pair, *Biosens. Bioelectron.* 192 (2021) 113488–113493, <https://doi.org/10.1016/j.bios.2021.113488>.
- [29] A. Paudics, D. Hessz, M. Bojtár, I. Bitter, V. Horváth, M. Kállay, M. Kubinyi, A pillararene-based indicator displacement assay for the fluorescence detection of vitamin B1, *Sens. Actuators B Chem.* 369 (2022) 132364–132371, <https://doi.org/10.1016/j.snb.2022.132364>.
- [30] A.F. Sierra, D. Hernandez-Alonso, M.A. Romero, J.A. Gonzalez-Delgado, U. Pischel, P. Ballester, Optical supramolecular sensing of creatinine, *J. Am. Chem. Soc.* 142 (2020) 4276–4284, <https://doi.org/10.1021/jacs.9b12071>.
- [31] Y.M. Zhang, Y.H. Liu, Y. Liu, Cyclodextrin-based multistimuli-responsive supramolecular assemblies and their biological functions, *Adv. Mater.* 32 (2020) 1806158–1806176, <https://doi.org/10.1002/adma.201806158>.
- [32] J. Guo, J. Hou, J. Hu, Y. Geng, M. Li, H. Wang, J. Wang, Q. Luo, Recent advances in beta-cyclodextrin-based materials for chiral recognition, *Chem. Commun.* 59 (2023) 9157–9166, <https://doi.org/10.1039/dccc01962d>.
- [33] J. Wankar, N.G. Kotla, S. Gera, S. Rasala, A. Pandit, Y.A. Rochev, Recent advances in host-guest self-assembled cyclodextrin carriers: Implications for responsive drug delivery and biomedical engineering, *Adv. Funct. Mater.* 30 (2020) 1909049–1909075, <https://doi.org/10.1002/adfm.201909049>.
- [34] C. Yang, N. Spinelli, S. Perrier, E. Defrancq, E. Peyrin, Macrocyclic host-dye reporter for sensitive sandwich-type fluorescent aptamer sensor, *Anal. Chem.* 87 (2015) 3139–3143, <https://doi.org/10.1021/acs.analchem.5b00341>.
- [35] C. Tu, W. Wu, W. Liang, D. Zhang, W. Xu, S. Wan, W. Lu, C. Yang, Host-guest complexation-induced aggregation based on pyrene-modified cyclodextrins for improved electronic circular dichroism and circularly polarized luminescence, *Angew. Chem. Int. Ed.* 61 (2022) 202203541–202203545, <https://doi.org/10.1002/anie.202203541>.
- [36] H.L. Guo, X.F. Wang, Q.Y. Qian, F.B. Wang, X.H. Xia, A green approach to the synthesis of graphene nanosheets, *ACS Nano* 3 (2009) 2653–2659, <https://doi.org/10.1021/nn900227d>.
- [37] C. Liu, K. Wang, S. Luo, Y. Tang, L. Chen, Direct electrodeposition of graphene enabling the one-step synthesis of graphene-metal nanocomposite films, *Small* 7 (2011) 1203–1206, <https://doi.org/10.1002/smll.201002340>.
- [38] L. Zheng, S. Wu, X. Lin, L. Nie, L. Rui, X. Yang, Preparation and characterization of a novel β-cyclodextrin modified poly(n-acetylalanine) film, *Macromolecules* 35 (2002) 6174–6177, <https://doi.org/10.1021/ma011663j>.
- [39] G. Zhu, L. Wu, X. Zhang, W. Liu, X. Zhang, J. Chen, A new dual-signalling electrochemical sensing strategy based on competitive host-guest interaction of a

- β -cyclodextrin/poly(n-acetylaniline)/graphene-modified electrode: sensitive electrochemical determination of organic pollutants, *Chem. Eur. J.* 19 (2013) 6368–6373, <https://doi.org/10.1002/chem.201204635>.
- [40] W. Yang, R.Y. Lai, Comparison of the stem-loop and linear probe-based electrochemical DNA sensors by alternating current voltammetry and cyclic voltammetry, *Langmuir* 27 (2011) 14669–14677, <https://doi.org/10.1021/la203015v>.
- [41] Y. Wang, G. Ning, Y. Wu, S. Wu, B. Zeng, G. Liu, X. He, K. Wang, Facile combination of beta-cyclodextrin host-guest recognition with exonuclease-assistant signal amplification for sensitive electrochemical assay of ochratoxin A, *Biosens. Bioelectron.* 124–125 (2019) 82–88, <https://doi.org/10.1016/j.bios.2018.10.007>.
- [42] Y. Wang, G. Ning, H. Bi, Y. Wu, G. Liu, Y. Zhao, A novel ratiometric electrochemical assay for ochratoxin a coupling Au nanoparticles decorated mos₂ nanosheets with aptamer, *Electrochim. Acta* 285 (2018) 120–127, <https://doi.org/10.1016/j.electacta.2018.07.195>.
- [43] Z. Gong, Z. Zhang, Cyclodextrin-based optosensor for the determination of quinine, *Fresenius J. Anal. Chem.* (1997) 1093–1096, <https://doi.org/10.1007/s002160050311>.
- [44] J. Wojcik, A. Ejchart, M. Nowakowski, Shape adaptation of quinine in cyclodextrin cavities: NMR studies, *Phys. Chem. Chem. Phys.* 21 (2019) 6925–6934, <https://doi.org/10.1039/c9cp00590k>.
- [45] A. Khodadoust, N. Nasirizadeh, R.A. Taheri, M. Dehghani, M. Ghanei, H. Bagheri, A ratiometric electrochemical DNA-biosensor for detection of mir-141, *Mikrochim. Acta* 189 (2022) 213–224, <https://doi.org/10.1007/s00604-022-05301-w>.
- [46] Y. Liu, C. Wang, C. Zhang, R. Chen, B. Liu, K. Zhang, Nonenzymatic multiamplified electrochemical detection of medulloblastoma-relevant micrnas from cerebrospinal fluid, *ACS Sens.* 7 (2022) 2320–2327, <https://doi.org/10.1021/acssensors.2c00956>.
- [47] C. Zhu, D. Liu, Y. Li, S. Ma, M. Wang, T. You, Hairpin DNA assisted dual-ratiometric electrochemical aptasensor with high reliability and anti-interference ability for simultaneous detection of aflatoxin B1 and ochratoxin A, *Biosens. Bioelectron.* 174 (2021) 112654–112661, <https://doi.org/10.1016/j.bios.2020.112654>.
- [48] V. Vivier, M.E. Orazem, Impedance analysis of electrochemical systems, *Chem. Rev.* 122 (2022) 11131–11168, <https://doi.org/10.1021/acs.chemrev.1c00876>.